

A Mixed-Integer Programming Approach for an Extended Fixed Route Hybrid Electric Aircraft Charging Problem

Anthony Deschênes¹^a, Raphaël Boudreault²^b, Jonathan Gaudreault¹^c and Claude-Guy Quimper¹^d

¹Department of Computer Science and Software Engineering, Université Laval, Québec, Canada

²Thales, Québec, Canada

anthony.deschenes.1@ulaval.ca, raphael.boudreault@thalesgroup.com, {jonathan.gaudreault, claud-guy.quimper}@ift.ulaval.ca

Keywords: Energy Management, Hybrid Electric Aircraft, Air Mobility, Mixed-Integer Programming, Dynamic Programming, Optimization, FRHACP


Abstract: Air mobility is rapidly transitioning towards hybrid electric aircraft. In the context of multi-flight missions, aircraft operators will need to consider numerous infrastructure and operational constraints in their planning, where predicting energy usage is critical. This problem is introduced in previous work as the *Fixed Route Hybrid Electric Aircraft Charging Problem* (FRHACP) and a Dynamic Programming (DP) approach is proposed. It consists of deciding a cost-optimal charging, refueling, and hybridization strategy for a given aircraft route. In this paper, we introduce an extended version of this problem with additional constraints and soft schedule requirements. We then propose a Mixed-Integer Programming (MIP) approach to solve it and compare its performance against an updated DP approach on a benchmark of 10 realistic instances. Results demonstrate that MIP consistently produces superior solutions than DP, both with and without gradient descent post-treatment, achieving average cost reductions of 145\$ (1.7%) and 377\$ (4.3%), respectively. However, it increases on average the solving time. We finally discuss the benefits and drawbacks of both approaches, with a particular emphasis on the scalability of DP through additional experiments.


1 INTRODUCTION


Historically, air transportation has heavily relied on aircraft propelled by combustion engines that utilize non-renewable fossil fuels. However, in the past years, there has been a growing interest in exploring alternative propulsion systems aiming to reduce greenhouse gas emissions from aviation. For that purpose, electric-powered aircraft, including hybrid electric aircraft combining internal combustion engines with electric power sources, have been proposed. It is anticipated that these aircraft will play a crucial role in the future of air transportation, operating across a variety of multi-flight missions, including on-demand services of varying length and duration (Ansell and Haran, 2020).


Nevertheless, the adoption of electric propulsion

introduces several complex challenges. Beyond flight path planning, effectively managing energy consumption throughout entire missions is critical. This includes considering aircraft specifications, infrastructure availability, security requirements, and scheduling priorities. Such considerations are particularly important from a planning standpoint given the current non-negligible and non-linear duration of electricity charging (Deschênes et al., 2022; Montoya et al., 2017). Operators must make informed decisions regarding refueling and charging at each mission terminal. Additionally, the consideration of hybridization introduces decisions on the energy source to use (electricity and/or fuel) during each flight leg. These decisions require consumption predictions from non-linear energy models depending among others on vehicle characteristics, speed, mass, and temperature (Sun et al., 2020; De Cauwer et al., 2017; Ansarey et al., 2014; Deschênes et al., 2020a). Ultimately, the main goal for operators is to minimize overall mission costs by ensuring efficient energy utilization.

^a <https://orcid.org/0000-0002-6670-6837>

^b <https://orcid.org/0000-0002-5602-7515>

^c <https://orcid.org/0000-0001-5493-8836>

^d <https://orcid.org/0000-0002-5899-0217>

In previous work by (Deschênes et al., 2023), this problem is introduced as the *Fixed Route Hybrid Electric Aircraft Charging Problem* (FRHACP) and a DP approach is proposed. In this paper, we introduce an extended version of this problem with additional constraints and soft schedule requirements and propose a MIP approach to solve it. Section 2 recalls the FRHACP definition. Section 3 introduces the extended problem and relates it to its original formulation. Section 4 presents how we update the DP approach for the extended problem, while the proposed MIP model is outlined in Section 5. The two approaches are evaluated and compared in Section 6 on a benchmark of 10 realistic instances, followed by a conclusion suggesting directions for future work.

In summary, the contributions of this paper are the following:

- A new extension of the FRHACP with additional constraints and a soft schedule;
- An updated DP approach that solves this extended problem;
- A new MIP model that solves this extended problem to optimality;
- A comparative analysis of the approaches' solutions and their computation time on a benchmark of 10 realistic instances;
- A scalability analysis of the proposed approaches on larger instances.

2 The Fixed Route Hybrid electric Aircraft Charging Problem (FRHACP)

The FRHACP is introduced by (Deschênes et al., 2023). It consists of deciding a cost-optimal charging, refueling and hybridization strategy for a given aircraft route in a multi-flight mission setting. Formally, a mission is defined as a fixed route $r := (n_1, n_2, \dots, n_{|\mathcal{N}|})$ of successive *nodes* $n_i \in \mathcal{N}$. Each node from the route is either a *terminal* from set \mathcal{T} or a *waypoint* from set \mathcal{W} ($\mathcal{N} := \mathcal{T} \cup \mathcal{W}$), with $n_1, n_{|\mathcal{N}|} \in \mathcal{T}$. A terminal is typically an airport, where facilities are available to refuel and charge the aircraft. Between consecutive terminals, the route is defined by waypoints, typically reference points in the air that must be part of the aircraft trajectory. *Legs* are defined as the route segments connecting two consecutive nodes, with $\mathcal{L} := \{(n_i, n_{i+1}) : i = 1, \dots, |\mathcal{N}| - 1\}$.

The FRHACP asks to decide how much to refuel and charge the aircraft at each terminal. These decisions are limited by security margins, physical ca-

Table 1: Parameters required by an instance of the FRHACP

Parameter	Description
s_1	Initial state of charge at the origin (%).
f_1	Initial fuel quantity at the origin (L).
t_1	Initial time at the origin (h).
s^{\min}	Minimal state of charge (%).
s^{\max}	Maximal state of charge (%).
f^{\min}	Minimal fuel quantity (L).
f^{\max}	Maximal fuel quantity (L).
$t_{\tau}^{\mathcal{D}}$	Scheduled departure time at terminal $\tau \in \mathcal{T}$ (h).
$\alpha_{\tau}^e(s_1, s_2)$	Function of the time to charge (h) from state of charge s_1 (%) to s_2 (%) at terminal $\tau \in \mathcal{T}$, defined for $s_1 \geq s_2$.
α^f	Refueling rate of the aircraft (L/h).
m^f	Fuel mass (kg/L).
m^a	Empty aircraft mass (kg).
m_l^p	Payload mass on leg $l \in \mathcal{L}$ (kg).
d_l	Travel distance on leg $l \in \mathcal{L}$ (km).
v_l	Aircraft speed on leg $l \in \mathcal{L}$ (km/h).
$\delta_l^e(d, m)$	Function of the electricity consumption (%) given the distance d (km) and the mass m (kg) on leg $l \in \mathcal{L}$.
$\delta_l^f(d, m)$	Function of the fuel consumption (L) given the distance d (km) and the mass m (kg) on leg $l \in \mathcal{L}$.
c_{τ}^e	Electricity cost at terminal $\tau \in \mathcal{T}$ (\$/%).
c_{τ}^f	Fuel cost at terminal $\tau \in \mathcal{T}$ (\$/L).

capacity, and hard schedule constraints on the departure time. The time needed to charge the aircraft battery at a terminal is encoded as a function dependent on the initial and final states of charge, usually non-linear (Deschênes et al., 2022; Montoya et al., 2017), while the refueling duration is given by a constant rate. Hybridization decisions on the energy source to use (electricity and/or fuel) during each leg is encoded as the traveled distance using fuel first. This is based on the hypotheses that fuel has a non-negligible mass, which is an important non-linear factor in energy consumption prediction (Sun et al., 2020; De Cauwer et al., 2017; Ansarey et al., 2014; Deschênes et al., 2020a), and that using fuel first is the optimal energy management strategy on a leg (Pinto Leite and Voskuijl, 2020). Thus, fuel and electricity consumption models are encoded as functions dependent on the traveled distance and the total mass. These may include other physical parameters, such as speed, altitude, and trajectory angle, but are assumed constant on a given leg. In summary, a FRHACP instance requires the parameters listed in Table 1.

The FRHACP can naturally be seen as an adaptation of the *Fixed Route Electric Vehicle Charging Problem* (FRVCP), introduced by (Montoya et al., 2017), to the context of hybrid electric aircraft. This problem has been extended with non-linear energy

management by (Deschênes et al., 2020b), and MIP approaches have been proposed to solve both formulations. In fact, the FRVCP can be seen as a sub-problem of the *Electric Vehicle Routing Problem* (EVRP) introduced by (Lin et al., 2016). Their work highlights that payload, and consequently vehicle mass, has a significant impact on energy consumption of electric vehicles. The EVRP has also been extended to handle hybrid electric vehicles, with mainly MIP approaches used to solve the new problems (Mancini, 2017; Seyfi et al., 2022; Zhen et al., 2020), as well as heuristics (Seyfi et al., 2022; Zhen et al., 2020; Yu et al., 2017).

3 THE EXTENDED FRHACP

We now introduce an extension of the FRHACP described in Section 2. The main difference lies in the schedule management, where now the mission schedule satisfaction is encoded as soft constraints on the arrival and departure times at each terminal. Thus, in the new problem, time is an additional dimension to consider, while monetary costs are associated on the deviation from the given scheduled times. Furthermore, it now allows a decision of *waiting*, i.e. to perform other tasks than charging and refueling at a terminal, which can be constrained (e.g., for maintenance purposes). A maximal charging duration and fuel availability can be specified as constraints at each terminal, while the availability of charging/refueling facilities can also vary. Finally, in this extended problem, a specific source of energy to use can be enforced on a given leg (e.g., to enforce that taxi phases use electricity). Table 2 presents the additional parameters required by an extended FRHACP instance as well as the value each parameter needs to obtain an original FRHACP instance.

4 UPDATED DYNAMIC PROGRAMMING AND HEURISTICS APPROACHES

(Deschênes et al., 2023) propose a DP algorithm to solve the FRHACP, which minimizes fuel consumption and is optimal under certain assumptions, including one that requires that fuel costs are the same at each terminal. To relax this assumption, they propose a gradient descent post-treatment that keeps the optimality when fuel costs vary, DP+GD. They also proposed two heuristics: one that prioritizes fuel usage, *Fuel First* (FF-H), and one that greedily prioritizes

Table 2: Additional parameters required by an instance of the extended FRHACP and their value needed to obtain an instance of FRHACP

Parameter	Description	Value
$t_{\tau}^{\mathcal{A}}$	Scheduled arrival time at terminal $\tau \in \mathcal{T}$ (h).	N/A
$c_{\tau}^{< t_{\tau}^{\mathcal{A}}}$	Cost of arriving earlier than the scheduled arrival time at terminal $\tau \in \mathcal{T}$ (\$/h).	N/A
$c_{\tau}^{> t_{\tau}^{\mathcal{A}}}$	Cost of arriving later than the scheduled arrival time at terminal $\tau \in \mathcal{T}$ (\$/h).	N/A
$c_{\tau}^{< t_{\tau}^{\mathcal{D}}}$	Cost of departing earlier than the scheduled departure time at terminal $\tau \in \mathcal{T}$ (\$/h).	∞
$c_{\tau}^{> t_{\tau}^{\mathcal{D}}}$	Cost of departing later than the scheduled departure time at terminal $\tau \in \mathcal{T}$ (\$/h).	∞
$\Delta t_{\tau}^{\text{wait}, \min}$	Minimal waiting duration at terminal $\tau \in \mathcal{T}$ (h).	0
$\Delta t_{\tau}^{s, \max}$	Maximal charging duration at terminal $\tau \in \mathcal{T}$ (h).	∞
Δf_{τ}^{\max}	Available fuel quantity at terminal $\tau \in \mathcal{T}$ (L).	∞
can_{τ}^s	1 if we can charge at terminal $\tau \in \mathcal{T}$, else 0.	1
can_{τ}^f	1 if we can refuel at terminal $\tau \in \mathcal{T}$, else 0.	1
allowed_l^s	1 if we can use electricity on leg $l \in \mathcal{L}$, else 0.	1
allowed_l^f	1 if we can use fuel on leg $l \in \mathcal{L}$, else 0.	1

electricity usage by always burning the fuel before using the electricity to minimize the aircraft weight when using the electricity, *Maximum Battery Usage* (MB-H). Formal descriptions of the DP algorithms and the heuristics are provided by (Deschênes et al., 2023). To solve the extended FRHACP introduced in Section 3, we update their DP approach. The modifications and new assumptions are as follows:

- Soft schedule is not handled. Scheduled times are thus strictly considered as in the FRHACP;
- Minimal waiting and maximal charging durations are handled when constructing the route solution;
- Available fuel quantities are ensured by limiting the recurrence returned value. Since DP minimizes the fuel usage, this handles the majority of cases. Degenerated cases would cause unfeasibility;
- Availability of charging/refueling facilities is directly handled by the two above items;
- Enforced energy source usage on legs is handled by fixing the tested hybridization decisions to either fully electric or fully fuel.

As a result, hypotheses for optimality no longer hold, and the solutions produced by the DP approach, with

or without the gradient descent post-treatment, are no longer guaranteed to be optimal. With a similar reasoning, the heuristics *Fuel First* and *Maximum Battery Usage*, can be updated to solve the extended FRHACP.

The DP approach depends on two hyperparameters: the number of sampled states of charge to create the interpolations, \tilde{s} , and the number of tested distance decisions for the hybridization, \tilde{h} . It has been shown that both of these hyperparameters have a linear impact on its running time (Deschênes et al., 2023).

5 PROPOSED MIXED-INTEGER PROGRAMMING MODEL

This section outlines the proposed MIP model in our approach to solve the extended FRHACP described in Section 3.

5.1 Variables

As for the FRHACP, the main decision variables for the extended problem are related to the charging and refueling durations/quantities at each terminal. In addition, new variables are related to the waiting duration at each terminal in order to handle soft schedule requirements and time constraints. Finally, hybridization is still encoded via traveled distance using each energy source. These variables, as well as intermediate variables used by the MIP model, are presented in Table 3 along with their initial domain based on parameters from Tables 1 and 2.

5.2 Objective

The objective is to minimize the total cost of the multi-flight mission. It includes energy-related costs (charging and refueling), as in the FRHACP, but also costs induced by deviation from the scheduled arrival and departure times:

$$\min \sum_{\tau \in \mathcal{T}} \left[c_{\tau}^s (S_{\tau}^{\mathcal{D}} - S_{\tau}^{\mathcal{A}}) + c_{\tau}^f (F_{\tau}^{\mathcal{D}} - F_{\tau}^{\mathcal{A}}) + C_{\tau}^{<I^{\mathcal{A}}} + C_{\tau}^{>I^{\mathcal{A}}} + C_{\tau}^{<I^{\mathcal{D}}} + C_{\tau}^{>I^{\mathcal{D}}} \right].$$

5.3 Constraints

The constraints of the MIP model are presented below. We use M as a sufficiently large constant. Constraints (1) set the initial conditions at the first terminal $n_1 \in \mathcal{T}$.

$$S_{n_1}^{\mathcal{A}} = s_1, F_{n_1}^{\mathcal{A}} = f_1, T_{n_1}^{\mathcal{A}} = t_1 \quad (1)$$

Table 3: Variables of the MIP model and their initial domain

Variable	Domain	Description
ΔT_{τ}^s	$[0, \Delta_{\tau}^{s, \max}]$	Charging duration at terminal $\tau \in \mathcal{T}$ (h).
ΔT_{τ}^f	$[0, \frac{1}{\alpha^f} \cdot \Delta f_{\tau}^{\max}]$	Refueling duration at terminal $\tau \in \mathcal{T}$ (h).
$\Delta T_{\tau}^{\text{wait}}$	$[\Delta_{\tau}^{\text{wait}, \min}, \infty]$	Waiting duration at terminal $\tau \in \mathcal{T}$ (h).
D_l^s	$[0, d_l]$	Traveled distance using electricity on leg $l \in \mathcal{L}$ (km).
D_l^f	$[0, d_l]$	Traveled distance using fuel on leg $l \in \mathcal{L}$ (km).
$S_n^{\mathcal{A}}$	$[s_{\min}, s_{\max}]$	Arrival state of charge at node $n \in \mathcal{N}$ (%).
$S_n^{\mathcal{D}}$	$[s_{\min}, s_{\max}]$	Departure state of charge at node $n \in \mathcal{N}$ (%).
$F_n^{\mathcal{A}}$	$[f_{\min}, f_{\max}]$	Arrival fuel quantity at node $n \in \mathcal{N}$ (L).
$F_n^{\mathcal{D}}$	$[f_{\min}, f_{\max}]$	Departure fuel quantity at node $n \in \mathcal{N}$ (L).
M_l^s	$[m^a, \infty]$	Mass of the aircraft when using electricity on leg $l \in \mathcal{L}$ (kg).
M_l^f	$[m^a, \infty]$	Mass of the aircraft when using fuel on leg $l \in \mathcal{L}$ (kg).
ΔT_l^s	$[0, d_l/v_l]$	Traveled duration using electricity on leg $l \in \mathcal{L}$ (h).
ΔT_l^f	$[0, d_l/v_l]$	Traveled duration using fuel on leg $l \in \mathcal{L}$ (h).
$T_n^{\mathcal{A}}$	$[t_1, \infty]$	Arrival time at node $n \in \mathcal{N}$ (h).
$T_n^{\mathcal{D}}$	$[t_1, \infty]$	Departure time at node $n \in \mathcal{N}$ (h).
$C_{\tau}^{<I^{\mathcal{A}}}$	$[0, \infty]$	Total cost for arriving early at terminal $\tau \in \mathcal{T}$ (\$).
$C_{\tau}^{>I^{\mathcal{A}}}$	$[0, \infty]$	Total cost for arriving late at terminal $\tau \in \mathcal{T}$ (\$).
$C_{\tau}^{<I^{\mathcal{D}}}$	$[0, \infty]$	Total cost for departing early at terminal $\tau \in \mathcal{T}$ (\$).
$C_{\tau}^{>I^{\mathcal{D}}}$	$[0, \infty]$	Total cost for departing late at terminal $\tau \in \mathcal{T}$ (\$).

Constraints (2) define the relationship between the states of charge and the charging duration at a terminal, while constraints (3) allow charging only if facilities are available. Similarly, constraints (4) ensure that the refueling duration at a terminal is proportional to the aircraft refueling rate, while constraints (5) allow refueling only if facilities are available.

$$\Delta T_{\tau}^s = \alpha_{\tau}^s (S_{\tau}^{\mathcal{A}} - S_{\tau}^{\mathcal{D}}) \quad \forall \tau \in \mathcal{T} \quad (2)$$

$$\Delta T_{\tau}^s \leq M \cdot \text{can}_{\tau}^s \quad \forall \tau \in \mathcal{T} \quad (3)$$

$$\Delta T_{\tau}^f = \frac{1}{\alpha^f} (F_{\tau}^{\mathcal{D}} - F_{\tau}^{\mathcal{A}}) \quad \forall \tau \in \mathcal{T} \quad (4)$$

$$\Delta T_{\tau}^f \leq M \cdot \text{can}_{\tau}^f \quad \forall \tau \in \mathcal{T} \quad (5)$$

By assumption, constraints (6) enforce that charging, refueling, and waiting are not allowed at any way-

point.

$$S_w^{\mathcal{D}} = S_w^{\mathcal{A}}, \quad F_w^{\mathcal{D}} = F_w^{\mathcal{A}}, \quad T_w^{\mathcal{D}} = T_w^{\mathcal{A}} \quad \forall w \in \mathcal{W} \quad (6)$$

To encode the hybridization decisions on each flight leg, constraints (7) to (9) define the relationship between distance and duration variables according to given distance and speed. Additionally, the ability to use electricity and/or fuel on a leg is encoded via constraints (10) and (11).

$$D_l^s = v_l \Delta T_l^s \quad \forall l \in \mathcal{L} \quad (7)$$

$$D_l^f = v_l \Delta T_l^f \quad \forall l \in \mathcal{L} \quad (8)$$

$$\Delta T_l^s + \Delta T_l^f = \frac{d_l}{v_l} \quad \forall l \in \mathcal{L} \quad (9)$$

$$(1 - \text{allowed}_l^s) \Delta T_l^s \leq 0 \quad \forall l \in \mathcal{L} \quad (10)$$

$$(1 - \text{allowed}_l^f) \Delta T_l^f \leq 0 \quad \forall l \in \mathcal{L} \quad (11)$$

Constraints (12) define the mass of the aircraft at the start of each leg according to its initial fuel quantity. Then, after using the fuel first with this mass, constraints (13) compute the updated mass of the aircraft according to its final fuel quantity to be considered for the electric part of the leg.

$$M_{l_i}^f = m^a + m_{l_i}^p + m^f F_{n_i}^{\mathcal{D}} \quad \forall l_i := (n_i, n_{i+1}) \in \mathcal{L} \quad (12)$$

$$M_{l_i}^s = m^a + m_{l_i}^p + m^f F_{n_{i+1}}^{\mathcal{A}} \quad \forall l_i := (n_i, n_{i+1}) \in \mathcal{L} \quad (13)$$

Constraints (14) and (15) define the variation in state of charge and fuel quantity, from a leg departure node to its arrival node, originating from energy consumption.

$$S_{n_{i+1}}^{\mathcal{A}} = S_{n_i}^{\mathcal{D}} - \delta_{l_i}^s(M_{l_i}^s, D_{l_i}^s), \quad \forall l_i := (n_i, n_{i+1}) \in \mathcal{L} \quad (14)$$

$$F_{n_{i+1}}^{\mathcal{A}} = F_{n_i}^{\mathcal{D}} - \delta_{l_i}^f(M_{l_i}^f, D_{l_i}^f), \quad \forall l_i := (n_i, n_{i+1}) \in \mathcal{L} \quad (15)$$

Constraints (16) encode the departure time from a terminal, which is defined by the arrival time, the charging and refueling durations, and the waiting duration. Constraints (17) encode the arrival time at a node according to its incoming leg duration.

$$T_{\tau}^{\mathcal{D}} = T_{\tau}^{\mathcal{A}} + \Delta T_{\tau}^s + \Delta T_{\tau}^f + \Delta T_{\tau}^{\text{wait}} \quad \forall \tau \in \mathcal{T} \quad (16)$$

$$T_{n_{i+1}}^{\mathcal{A}} = T_{n_i}^{\mathcal{D}} + \frac{d_{l_i}}{v_{l_i}} \quad \forall l_i := (n_i, n_{i+1}) \in \mathcal{L} \quad (17)$$

Finally, constraints (18) to (21) relate the schedule costs to their associated time variable.

$$C_{\tau}^{<I^{\mathcal{A}}} \geq c_{\tau}^{<I^{\mathcal{A}}} (t_{\tau}^{\mathcal{A}} - T_{\tau}^{\mathcal{A}}) \quad \forall \tau \in \mathcal{T} \quad (18)$$

$$C_{\tau}^{>I^{\mathcal{A}}} \geq c_{\tau}^{>I^{\mathcal{A}}} (T_{\tau}^{\mathcal{A}} - t_{\tau}^{\mathcal{A}}) \quad \forall \tau \in \mathcal{T} \quad (19)$$

$$C_{\tau}^{<I^{\mathcal{D}}} \geq c_{\tau}^{<I^{\mathcal{D}}} (t_{\tau}^{\mathcal{D}} - T_{\tau}^{\mathcal{D}}) \quad \forall \tau \in \mathcal{T} \quad (20)$$

$$C_{\tau}^{>I^{\mathcal{D}}} \geq c_{\tau}^{>I^{\mathcal{D}}} (T_{\tau}^{\mathcal{D}} - t_{\tau}^{\mathcal{D}}) \quad \forall \tau \in \mathcal{T} \quad (21)$$

5.4 Function Linearizations

Following the methodology of (Deschênes et al., 2020b), the non-linear charging functions $\alpha_{\tau}^s(s_1, s_2)$ are approximated using multiple linear functions that each add a binary variable to the model, for each terminal $\tau \in \mathcal{T}$.

The non-linear electricity and fuel consumption functions, $\delta_l^s(d, m)$ and $\delta_l^f(d, m)$, both depend on distance and mass decisions. We approximate these multidimensional functions in the MIP model using the method of (Misener and Floudas, 2010), which depends on a grid sampling. This leads to two hyperparameters: the number of points in the grid for the distance dimension, \tilde{d} , and for the mass dimension, \tilde{m} . The approximation adds $\tilde{d} + \tilde{m}$ binary variables for each leg $l \in \mathcal{L}$. It is known that the finer the grid, the better approximations will be, but harder it will be to solve.

6 EXPERIMENTS

The main objective of the experiments is to compare the proposed MIP approach from Section 5 with the updated DP approach from Section 4, in terms of solving time and solution quality. This aims at evaluating the benefits and drawbacks of each approach.

6.1 Experimental Setup

We implemented the MIP model from Section 5 in the MiniZinc 2.8.3 language (Nethercote et al., 2007) and used CPLEX 22.1 for solving, with an optimal relative gap setting of $1e-10$. Based on the methods of (Deschênes et al., 2023), we implemented in Python 3.11 the updated DP, its gradient descent post-treatment (DP+GD), and the heuristics (FF-H, MB-H) as described in Section 4. The experiments were performed on an Intel Core i7-8750H CPU @ 2.20 GHz, 6 cores and 8 GB of RAM. In order to compare each method on the same basis, a simulation using the non-approximated functions is always performed as

Table 4: Description of the ten instances forming the dataset

Instance	$ \mathcal{T} $	$ \mathcal{W} $	Duration	Distance (km)	c^s (\$/kWh)	c^f (\$/L)
PN	4	59	4h30	2740	0.1397	1.46
TB	5	42	6h42	2812	0.1397	1.46
MS	6	30	7h22	2294	0.0533	[1.16, 1.25]
OT	7	43	9h34	4709	[0.0533, 0.1140]	[1.03, 1.28]
KT	7	47	10h45	5165	[0.0776, 0.1408]	[1.13, 1.38]
ST	6	52	13h10	6788	[0.0898, 0.1234]	[1.03, 1.37]
TV	6	64	14h36	8493	[0.0976, 0.1408]	[1.13, 1.44]
SK	7	107	16h33	9456	[0.0533, 0.1408]	[1.16, 1.44]
BK	10	72	16h46	8143	[0.0590, 0.1408]	[1.13, 1.44]
VT	5	49	11h17	5886	[0.0776, 0.1408]	[1.26, 1.41]

a post-treatment. Additionally, the MIP performs energy quantity corrections after the simulation to reduce its approximation errors and stay as close as possible to its original optimal solution.

6.2 Dataset

Our dataset consists of the four real-life inspired instances from (Deschênes et al., 2023), which were created from day-long sequences of aircraft commercial flights in Canada and France. Following a similar instance construction methodology, we augmented this dataset with six new instances (KT, ST, TV, SK, BK, and VT) inspired by real commercial flights in Canada. The resulting dataset is summarized in Table 4. Note that all costs are presented in CAD (\$). With the new instances, the number of terminals now varies from 4 to 10, with a number of waypoints between 30 and 107, and a traveled distance of up to 9456 km.

All instances suppose a *Cessna S550 Citation II* as the aircraft, which is augmented with a battery of 216 kWh, and has the specifications from (Deschênes et al., 2023). It relies on the OpenAP aircraft performance model (Sun et al., 2020) to predict the energy consumption as functions $\delta_l^s(d, m)$ and $\delta_l^f(d, m)$, using the fixed parameters of leg $l \in \mathcal{L}$. Since OpenAP doesn't handle consumption predictions while taxiing, we suppose the associated legs are fully electric and use instead a physical model for electric vehicles (De Cauwer et al., 2017). For the charging functions $\alpha_\tau^s(s_1, s_2)$, it uses for all terminals $\tau \in \mathcal{T}$ the non-linear charging function from (Deschênes et al., 2020b), approximated for the MIP by six linear functions minimizing the error in its exponential part.

Additionally, we suppose the following parameters for the extended FRHACP. We fix the scheduled arrival times using the departure times and the planned durations. The soft schedule costs are fixed for all terminals $\tau \in \mathcal{T}$ to $c_\tau^{<t^A} = 0.25\$/\text{min}$ and $c_\tau^{>t^A} = 20\$/\text{min}$. Some terminals do not have electricity charging stations, while every taxi leg is forced to be traveled using only electricity. For this benchmark, remaining parameters are set in a way that they

do not incur additional constraints.

6.3 Hyperparameters Optimization

Both MIP and DP have hyperparameters, affecting the solving time and the quality of the solution, that must be chosen. To ensure a fair comparison between the approaches, these hyperparameters should be selected using an objective methodology. Otherwise, manually selecting hyperparameters could lead to biased conclusions. Therefore, we split the dataset in a training set and a test set. The training set is used to determine a good combination of hyperparameters, while the test set is used to compute the results. In order to obtain a representative training set, we choose the instances with the most and least terminals and waypoints, i.e. PN, MS, SK, and BK. The test set contains the remaining six instances.

For each combination of hyperparameters, we run the approach (MIP or DP) on all instances of the training set. We then compute the average total cost and solving time over all training instances. Note that, for both approaches, we exclude from the solving time the calls to OpenAP. Finally, we generate Pareto fronts containing all compromises between the total cost and the solving time. Using the distance from the ideal point algorithm (Ehrgott and Tenfelde-Podehl, 2003), a combination of hyperparameters is chosen for each approach.

The MIP approach has two hyperparameters, \tilde{d} and \tilde{m} , as presented in Section 5.4. For both, we tested values ranging from 2 to 10, for a total of 81 combinations. Figure 1 presents the resulting Pareto front. The chosen combination of hyperparameters is point J, with $(\tilde{d}, \tilde{m}) = (2, 4)$.

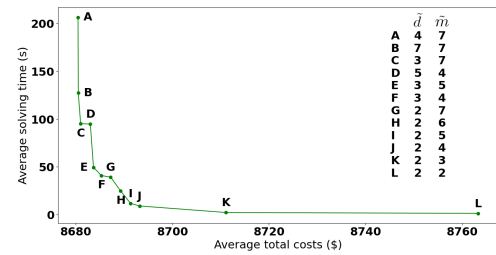


Figure 1: Resulting Pareto front for the MIP approach on the training set with tested hyperparameter combinations.

The DP approach has two hyperparameters, \tilde{s} and \tilde{h} , as presented in Section 4. For both, we tested values ranging from 10 to 100 with a step of 10, for a total of 100 combinations. Figure 2 presents the resulting Pareto front. The chosen combination of hyperparameters is point E, with $(\tilde{s}, \tilde{h}) = (40, 40)$.

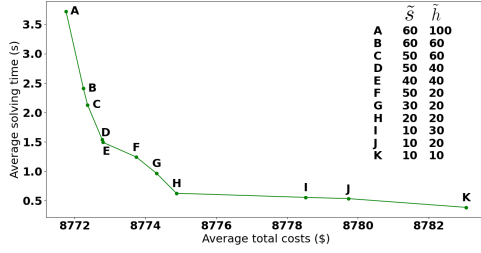


Figure 2: Resulting Pareto front for the DP approach on the training set with tested hyperparameter combinations.

6.4 Results

Table 5 presents the results of our experiments on the test set. For each method (DP, DP+GD, MIP, FF-H, MB-H) and each instance, we report the solving time as well as costs and consumed quantities of each energy source. The solving time is computed over 30 runs with a 95% confidence interval. We also distinguish the solving time of the algorithms (*Internal*) from the calls to OpenAP (*External*) since OpenAP can take a considerable amount of time to compute its predictions. The fuel costs do not vary in instance TB, thus the DP+GD method is omitted due to returning the same solution as DP.

For the solving time, we observe that MIP has on average a statistically lower total solving time compared to DP and DP+GD. However, DP and DP+GD have on average a statistically lower *internal* solving time than MIP, meaning that most of the time of these methods is inside external calls to OpenAP. This external time could *a priori* be reduced by using caching techniques or different external models. Thus, we can conclude that DP and DP+GD have globally a smaller solving time than MIP.

For the costs, we observe that MIP has the smallest total cost for all instances. Compared to DP, its total cost is on average 376.82\$ (4.31%) smaller, with a difference going from 53.94\$ (1.17%) to as much as 692.44\$ (7.39%). Compared to DP+GD, its total cost is on average 144.96\$ (1.67%) smaller, with a difference going from 17.80\$ (0.28%) to 502.78\$ (5.37%). Compared to the heuristics, MIP is on average 695.05\$ (8.75%) smaller than MB-H and 1135.91\$ (14.68%) smaller than FF-H, with a maximum reduction of 1443.75\$ (22.62%). For all instances, the cost reduction mainly comes from a greater electricity usage, with an increased electricity consumption and costs, to allow for a smaller fuel consumption. We also observe that, for most instances, MIP has larger schedule costs, implying that its higher electricity usage also comes from taking advantage of the soft schedule. Notably, it tends to ar-

rive earlier at terminals in order to increase its available charging time.

The MIP method always has the greatest electricity consumption of all the methods. This allows to reduce the fuel consumption on average by 119.2 L (1.79%) in comparison with DP+GD, with a reduction of up to 680.4 L (11.79%) compared to FF-H which focuses on using fuel as much as possible. Furthermore, DP has a smaller fuel consumption than MIP for two instances: OT (88.6 L, 1.58%) and ST (122.4 L, 1.39%). Thus, the optimal solution minimizing total costs is, for some instances, not always the solution that minimizes the fuel consumption.

6.5 Scalability Analysis

We tested the scalability of the proposed approaches by conducting an experimentation where the size of instances was artificially increased to a given number of terminals. For any instance, we can increase its size by appending at its end the same flights again up to any terminal in the instance. For example, instance PN with 4 terminals could be increased to 8 terminals by doing all the flights in its route twice. Thus, for all instances in the test set, we increased their size to 10, 15, 20, and 25 terminals and computed the average total solving time of each method with a computation timeout of 54 hours. Figure 3 presents the results as a semi-log plot of the average total solving time of each method given the number of terminals. We observe that MIP can only solve instances of up to 15 terminals in less than 20 minutes. In contrast, DP and DP+GD clearly show a smaller increase in solving time as the number of terminals increase and thus scale better than the MIP approach. DP shows a linear trend with a R^2 of 0.99. This is expected since (Deschênes et al., 2023) show that its time complexity is pseudo-linear with the number of nodes in the instance, which is directly proportional to the number of terminals. However, DP+GD shows an exponential trend with a R^2 of 0.99. This can be explained by the fact that the gradient descent post-treatment can take an exponential time to converge. Similarly, MIP clearly shows an exponential trend with a R^2 of 0.95 with an average total solving time higher than DP and DP+GD for 15 terminals and above. The MIP method on TB with 25 terminals reached the computation timeout of 54 hours with a relative gap of 0.14%.

6.6 Discussion

Results from Section 6 demonstrate that the MIP approach always yields better solutions than the DP approach, but that the latter has a smaller internal solv-

Table 5: Solving time of each instance in seconds — distinguished between internal (algorithms) and external (OpenAP) time — as well as costs and consumed quantities of energy. Results reported for the DP, DP+GD, MIP, FF-H, and MB-H methods

Instance	Method	Solving time (s)			Costs (\$)				Consumption	
		Internal	External	Total	Fuel	Electricity	Schedule	Total	Fuel (L)	Electricity (kWh)
TB	DP	0.63 ± 0.06	12.02 ± 0.48	12.65 ± 0.53	4517.18	142.25	0.77	4660.20	3117.2	683.1
	DP+GD	-	-	-	-	-	-	-	-	-
	MIP	4.42 ± 0.38	0.04 ± 0.00	4.46 ± 0.38	4448.19	152.85	5.21	4606.25	3066.8	732.2
	FF-H	0.00 ± 0.00	0.09 ± 0.01	0.08 ± 0.00	5421.53	0.78	0.77	5422.08	3739.8	3.4
	MB-H	0.02 ± 0.01	0.67 ± 0.03	0.69 ± 0.03	4817.62	124.51	0.77	4942.90	3319.5	572.2
OT	DP	0.66 ± 0.10	13.68 ± 0.59	14.34 ± 0.67	6577.00	94.67	3.22	6674.89	5533.3	1070.4
	DP+GD	0.82 ± 0.07	16.36 ± 0.55	17.18 ± 0.59	6301.30	94.66	3.22	6399.18	5648.1	1070.4
	MIP	1.68 ± 0.32	0.03 ± 0.00	1.71 ± 0.32	6280.22	96.88	4.28	6381.38	5621.9	1096.7
	FF-H	0.00 ± 0.00	0.09 ± 0.01	0.09 ± 0.01	7821.26	0.65	3.22	7825.14	6540.4	6.8
	MB-H	0.03 ± 0.01	0.80 ± 0.03	0.83 ± 0.03	7277.74	84.47	3.22	7365.44	5853.0	937.7
KT	DP	0.72 ± 0.11	15.31 ± 1.45	16.04 ± 1.54	7994.60	90.35	0.92	8085.87	6389.5	908.1
	DP+GD	1.00 ± 0.15	18.19 ± 1.79	19.19 ± 1.90	7795.95	89.54	0.92	7886.41	6428.2	902.4
	MIP	6.85 ± 0.26	0.04 ± 0.00	6.89 ± 0.26	7643.36	105.16	11.95	7760.47	6296.5	1039.1
	FF-H	0.00 ± 0.00	0.10 ± 0.01	0.10 ± 0.01	9011.19	0.52	0.92	9012.63	7193.5	4.7
	MB-H	0.04 ± 0.01	1.16 ± 0.03	1.20 ± 0.03	8304.79	73.99	0.92	8379.70	6636.8	723.6
ST	DP	0.87 ± 0.08	18.00 ± 1.27	18.87 ± 1.34	10558.1	50.86	0.52	10609.48	8669.0	488.9
	DP+GD	0.96 ± 0.10	19.81 ± 1.62	20.77 ± 1.71	9992.87	50.85	7.49	10051.21	8867.4	488.8
	MIP	4.66 ± 0.24	0.05 ± 0.00	4.72 ± 0.24	9887.23	54.24	2.28	9943.75	8791.4	526.4
	FF-H	0.00 ± 0.00	0.12 ± 0.01	0.11 ± 0.00	11129.70	0.60	0.52	11120.83	9133.1	5.6
	MB-H	0.05 ± 0.02	1.92 ± 0.03	1.97 ± 0.03	10740.08	39.77	0.52	10780.37	8823.9	366.1
TV	DP	1.10 ± 0.08	23.10 ± 1.00	24.20 ± 1.06	13032.49	79.02	0.61	13112.13	10612.5	670.2
	DP+GD	1.17 ± 0.09	24.21 ± 0.67	25.38 ± 0.73	12864.52	79.02	0.54	12944.08	10676.9	670.1
	MIP	6.02 ± 0.23	0.08 ± 0.02	6.10 ± 0.23	12786.33	87.03	8.88	12882.24	10606.7	732.5
	FF-H	0.00 ± 0.00	0.17 ± 0.01	0.17 ± 0.01	13892.69	0.46	0.61	13894.76	11303.8	3.6
	MB-H	0.09 ± 0.02	3.13 ± 0.06	3.22 ± 0.05	13334.31	68.58	0.61	13403.79	10856.6	544.7
VT	DP	0.86 ± 0.06	17.49 ± 0.68	18.35 ± 0.71	10013.70	29.87	20.15	10063.71	7398.5	336.1
	DP+GD	0.98 ± 0.08	19.65 ± 0.46	20.64 ± 0.53	9795.97	29.86	48.22	9874.05	7550.8	336.1
	MIP	2.22 ± 0.37	0.05 ± 0.00	2.26 ± 0.36	9286.90	68.34	16.03	9371.27	7189.0	686.8
	FF-H	0.00 ± 0.00	0.11 ± 0.02	0.10 ± 0.02	10470.68	0.30	15.45	10486.44	7744.1	2.7
	MB-H	0.04 ± 0.02	1.75 ± 0.27	1.79 ± 0.26	10204.31	23.71	15.45	10243.48	7532.0	260.7

ing time. This is expected, since the MIP is the only method capable of leveraging the soft schedule. Unlike other methods, which strictly adhere to the schedule and sometimes result in smaller charging windows, the MIP can choose to arrive earlier at a terminal, thus extending the available charging window. While this strategy incurs a cost for deviating from the schedule, it allows for a longer charging duration (which also incurs an additional cost), ultimately increasing the available electrical energy for the subsequent flight. This increase in electricity reduces

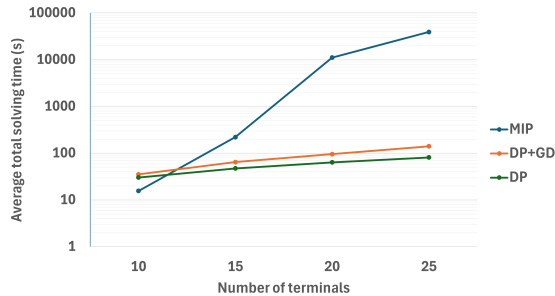


Figure 3: Semi-log plot of the average total solving time by DP, DP+GD, and MIP with respect to the number of terminals in the instances.

the fuel required for the next flight, thereby lowering fuel costs. The primary advantage of the MIP lies in its ability to identify scenarios where the reduction in fuel costs outweighs the combined costs associated with deviating from the schedule and increased electricity consumption. On the other hand, considering the soft schedule and all its different scenarios can cause higher solving time, thus explaining why the MIP has higher solving time than the other approaches.

Thus, each approach has its benefits and drawbacks. With an average reduction of 145\$ using the MIP method compared to the DP+GD method, aircraft operators in a real-life setting should evaluate if this cost reduction is profitable enough, notably when taking into account the costs of hosting such an approach (e.g., solver license costs and infrastructure). On the other hand, the DP approach has the advantage of having fewer hardware limitations (e.g., memory usage). Moreover, the MIP approach does not scale well on larger instances and could take days to solve, while DP could take less than 10 minutes.

On realistic instances, the MIP approach finds the optimal solution in less than 7 seconds, which makes it an interesting choice for a real-life planning con-

text. In addition, it is easier to improve and maintain, while it can take into consideration a wider range of constraints. It is thus easier to build on this approach to solve variants of the FRHACP and its extension. The MIP approach is also guaranteed to return an optimal solution (given its approximations), while the DP methods are only heuristics for this problem. We believe that greater variance in fuel, electricity and schedule costs could lead to greater cost differences between the approaches.

7 CONCLUSION

In this paper, we introduced an extended version of the FRHACP incorporating additional constraints and soft schedule requirements. To solve both the FRHACP and its extension, we proposed a MIP approach. Through a comparative analysis involving a benchmark of 10 realistic instances, we compared the MIP approach against an updated DP approach initially introduced in previous work for the FRHACP. Our findings consistently demonstrated that the MIP approach yields superior solutions than DP, both with and without gradient descent post-treatment, achieving average cost reductions of 145\$ (1.7%) and 377\$ (4.3%), respectively. However, we showed that it also requires a longer solving time compared to the DP approach. Furthermore, our analysis revealed that the MIP approach exhibits significantly lower scalability than its counterpart, thus each method has its advantages and limitations. Directions for future work include performing a sensitivity analysis on the impact of the different parameters, as well as considering a variable aircraft speed.

ACKNOWLEDGMENTS

This work received financial support from the Consortium for Research and Innovation in Aerospace in Quebec (CRIAQ) and the Mitacs Accelerate program. The authors would like to thank the many members of the Thales project team for their feedback on the problem definition and for the prototype implementation, especially Vanessa Simard for her contribution on the benchmark creation methodology.

REFERENCES

Ansarey, M., Shariat Panahi, M., Ziarati, H., and Mahjoob, M. (2014). Optimal energy management in a

- dual-storage fuel-cell hybrid vehicle using multi-dimensional dynamic programming. *Journal of Power Sources*, 250:359–371.
- Ansell, P. J. and Haran, K. S. (2020). Electrified airplanes: A path to zero-emission air travel. *IEEE Electrification Magazine*, 8(2):18–26.
- De Cauwer, C., Verbeke, W., Coosemans, T., Faid, S., and Van Mierlo, J. (2017). A data-driven method for energy consumption prediction and energy-efficient routing of electric vehicles in real-world conditions. *Energies*, 10(5):608.
- Deschênes, A., Boudreault, R., Simard, V., Gaudreault, J., and Quimper, C.-G. (2023). Dynamic programming for the fixed route hybrid electric aircraft charging problem. In Wu, W. and Guo, J., editors, *Combinatorial Optimization and Applications*, Lecture Notes in Computer Science, pages 354–365, Cham. Springer Nature Switzerland.
- Deschênes, A., Gaudreault, J., and Quimper, C.-G. (2022). Predicting real life electric vehicle fast charging session duration using neural networks. In *2022 IEEE Intelligent Vehicles Symposium (IV)*, pages 1327–1332.
- Deschênes, A., Gaudreault, J., Rioux-Paradis, K., and Redmont, C. (2020a). Predicting electric vehicle consumption: A hybrid physical-empirical model. *World Electric Vehicle Journal*, 11(1):2.
- Deschênes, A., Gaudreault, J., Vignault, L.-P., Bernard, F., and Quimper, C.-G. (2020b). The fixed route electric vehicle charging problem with nonlinear energy management and variable vehicle speed. In *2020 IEEE International Conference on Systems, Man, and Cybernetics (SMC)*, pages 1451–1458.
- Ehrgott, M. and Tenfelde-Podehl, D. (2003). Computation of ideal and Nadir values and implications for their use in MCDM methods. *European Journal of Operational Research*, 151(1):119–139.
- Lin, J., Zhou, W., and Wolfson, O. (2016). Electric vehicle routing problem. *Transportation Research Procedia*, 12:508–521.
- Mancini, S. (2017). The hybrid vehicle routing problem. *Transportation Research Part C: Emerging Technologies*, 78:1–12.
- Misener, R. and Floudas, C. A. (2010). Piecewise-linear approximations of multidimensional functions. *Journal of Optimization Theory and Applications*, 145(1):120–147.
- Montoya, A., Guéret, C., Mendoza, J. E., and Villegas, J. G. (2017). The electric vehicle routing problem with nonlinear charging function. *Transportation Research Part B: Methodological*, 103:87–110.
- Nethercote, N., Stuckey, P. J., Becket, R., Brand, S., Duck, G. J., and Tack, G. (2007). MiniZinc: Towards a standard CP modelling language. In Bessière, C., editor, *Principles and Practice of Constraint Programming – CP 2007*, Lecture Notes in Computer Science, pages 529–543, Berlin, Heidelberg. Springer. Website: <https://www.minizinc.org/>.
- Pinto Leite, J. P. S. and Voskuil, M. (2020). Optimal energy management for hybrid-electric aircraft. *Aircraft Engineering and Aerospace Technology*, 92(6):851–861.

- Seyfi, M., Alinaghian, M., Ghorbani, E., Çatay, B., and Sabbagh, M. (2022). Multi-mode hybrid electric vehicle routing problem. *Transportation Research Part E: Logistics and Transportation Review*, 166:102882.
- Sun, J., Hoekstra, J. M., and Ellerbroek, J. (2020). OpenAP: An open-source aircraft performance model for air transportation studies and simulations. *Aerospace*, 7(8):104.
- Yu, V. F., Redi, A. A. N. P., Hidayat, Y. A., and Wibowo, O. J. (2017). A simulated annealing heuristic for the hybrid vehicle routing problem. *Applied Soft Computing*, 53:119–132.
- Zhen, L., Xu, Z., Ma, C., and Xiao, L. (2020). Hybrid electric vehicle routing problem with mode selection. *International Journal of Production Research*, 58(2):562–576.